

# Neural Bistability and Amplification Mediated by NMDA Receptors: Analysis of Stationary Equations

Patrick A. Shoemaker<sup>a</sup>

<sup>a</sup>*Tanner Research, Inc., 825 South Myrtle Ave., Monrovia, CA 91941, USA*

Voice +1 626 471 9786

[pat.shoemaker@tanner.com](mailto:pat.shoemaker@tanner.com)

## Abstract

The macroscopic current/voltage relationship of NMDA receptor ion channels is nonmonotonic under physiological conditions, which can give rise to bistable and amplifying/facilitatory behavior in neurons and neural structures, supporting significant computational primitives. Conditions under which bistable regimes of operation prevail, and also general amplifying properties associated with active NMDA receptors, are examined in a single compartment enclosed by a cell membrane, and subsequently in cable-like dendrites under varying boundary conditions. Methodology consists of numerical and mathematical analyses of stationary versions of equations governing the electrical behavior of these systems. Bistability mediated by NMDA receptors requires interaction with other conductances in the membrane or cytoplasm, with particular importance attached to membrane potassium conductance, especially that of inward-rectifying potassium channels. A corollary conclusion is that coactivation of GABA<sub>B</sub> synaptic receptors or SK channels is a computationally powerful and sometimes necessary adjunct condition for NMDA receptor-mediated bistability. Neural multistability due to dendritic bistability is considered, including in the case of closely coupled dendrites. The characteristics of coactivation-dependent facilitation, and amplifying states in which NMDA receptor activation boosts the efficacy of other classes of synapses, are also described. Coactive inward-rectifying potassium channels are found to significantly affect the characteristics of such amplification.

Keywords: NMDA receptor; bistability; neuron; synapse; dynamical systems; GABA<sub>B</sub>; SK channels

**This is the web version of an article appearing in *Neurocomputing*:**

P.A. Shoemaker, "Neural Bistability and Amplification Mediated by NMDA Receptors: Analysis of Stationary Equations," *Neurocomputing*, doi: 10.1016/j.neucom.2011.04.01., 2011.

**The original publication is available at:**

<http://dx.doi.org/10.1016/j.neucom.2011.04.018>

## Introduction

This paper concerns electrical effects associated with the broadly distributed class of synaptic receptors (typically activated *in vivo* by the neurotransmitter glutamate) for which N-methyl-D-aspartate (NMDA) is an agonist. The macroscopic current-voltage relationship of the ion channels associated with NMDA receptors (NMDARs) is significantly nonlinear under physiological conditions [1,2], displaying a negative slope conductance regime due to (kinetically fast) magnesium blockade of the channels. This feature renders it capable of supporting bistable and amplifying behavior in conjunction with other membrane conductances and/or intracellular resistance.

Bistability – the capacity of a system to exist in either of two stable states when at equilibrium – is a phenomenon of interest in neuroscience because it provides a potential mechanism for short-term memory (NMDARs have in fact been implicated in ‘working memory’ in neuropsychology [3-5]), and more generally for a class of computations that implicitly require memory, such as temporal integration [6-8]. In physiological studies, evidence consistent with bistable behavior at the whole-neuron level has been observed in vertebrate neurons including Purkinje cells [9,10], pyramidal neurons [11-13], mitral cells in the olfactory bulb [14], entorhinal cortical cells [15], and various motoneurons [16-18]. Such behavior can arise as a network property in interconnected sets of neurons, due to positive feedback in combination with the saturating electrical characteristics of neurons (see, e.g., Li et al. [19]). However, it can also occur at a more primitive level, in individual neurons and their processes. The mechanism at this level is a nonmonotonic dependence of current flowing through the cell membrane on the potential difference across the membrane. There are several physiological mechanisms by which such a characteristic can arise, including the nonlinear macroscopic conductance of NMDARs, as well as the effects of slowly- or non-inactivating sodium [20,21] and calcium [22-24] currents. Of these, the NMDAR-based mechanism is particularly significant due to its direct control by synaptic inputs to a neuron.

In a bistable neuron or neural process, a regime exists in at least part of the structure in which the relationship between an injected current and local membrane potential is N-shaped and has three zeros of the current. The two zeros that occur with positive slope (those at the smallest and largest voltages) correspond to stable equilibria, and the middle zero to an unstable equilibrium. If the membrane current-voltage (I-V) relation itself has this characteristic, then when it encloses an isopotential electrical compartment, the system will be bistable with equilibrium potentials at the values corresponding to the stable zeros of the membrane current. I use the term ‘*bistable membrane I-V characteristic*’ as an abbreviated reference for a membrane current-voltage relationship of this sort, as distinct from, say, a nonmonotonic I-V relationship that has only a single zero. The latter case is still of interest with regard to bistability in non-isopotential neural models.

In addition to bistability, NMDARs can also mediate *amplifying effects* in nerve cells and neural processes; such effects have been noted in various cortical neurons [25-33], and implicated in the linearization of EPSP summation in CA1 pyramidal cells [34]. In qualitative terms, amplification associated with NMDARs is due to the fact that the more depolarized a neural process becomes, the greater the net depolarizing current contributed

by active NMDAR channels, while the local membrane potential remains within the negative conductance regime. This can increase the effectiveness of other classes of synaptic input; it can also result in pronounced superlinear effects in combination with voltage-gated ion channels [35]. In addition, because a fraction of this current is carried by calcium ions [36,37], an additional possible amplifying mechanism is the activation of calcium-dependent sodium channels [38,39] by increase of intracellular calcium. NMDAR-mediated amplification provides a local mechanism for nonlinear facilitation of perhaps equal possible importance to bistability. Various workers have commented on the potential computational significance of amplification associated with NMDARs [30,32,40,41], and Mel and colleagues have developed and studied computational algorithms based on it [32,42-44].

Schiller and Schiller [30] defined three putative regimes of the electrical effects associated with NMDARs: ‘boosting’, bistable, and ‘self-triggering’. The general conditions under which such regimes prevail, however, have apparently not been examined in detail. Lazarewicz et al. [41] considered bistability induced by NMDARs in combination with other membrane conductances, focusing on a particular structure (an electrically isolated dendritic segment with local synaptic activation along a fraction of its length), for specific combinations of geometric and electrical parameters. Korogod & Kulagina [45] modeled a dendrite with active NMDARs that terminates proximally on a soma, demonstrating the phenomenon that I call load-induced bistability, while Korogod & Chernetchenko [46] modeled a system consisting of two dendrites with NMDARs terminating on a common soma, demonstrating multistable behavior. Wolf et al. [47] modeled the specific role of NMDARs in the persistent ‘up’ and ‘down’ states observed in the medium spiny neuron of the nucleus accumbens.

This paper represents a first step toward a more general analysis of the electrical effects of NMDARs in concert with other membrane conductances. I focus on the analysis of stationary current-balance equations in order to characterize instantaneous dynamical regimes and examine the conditions supporting bistability and amplifying behavior. This is done with the recognition that dynamic rather than equilibrium conditions are prevalent in a nervous system, and that neural state depends on the dynamics of synaptic inputs as well as the kinetics of receptors and ion channels. When NMDARs are involved, any analysis of dynamic behavior is complicated by the fact that not just neural state, but dynamical regimes *themselves* may depend on synaptic inputs, and these regimes can change on a time scale comparable to changes in membrane potential. Dynamics are discussed briefly in the final section of the paper, but analysis of dynamic behavior is beyond its scope. The stationary analysis is nevertheless relevant, because it reveals the requirements for the existence *at any instant* of bistable dynamics, as well as other characteristics that affect neural behavior under nonequilibrium conditions. For example, the presence of two *basins of attraction* in the state space of a system can be inferred when stationary analysis indicates the presence of two stable equilibria, and this is relevant even if such equilibria are never reached. In such a system, small differences in initial conditions or external perturbations can influence the system to ‘jump’ from one basin to the other, resulting in significantly different paths of evolution in the state space.

The analysis herein focuses primarily on the electrical effects associated with the interaction between NMDARs, resting conductance, and synaptically-activated

conductances – the proximal causes of changes in the electrical state of the neuron from its resting condition. Of particular significance is interaction with the inward-rectifying potassium (Kir) channels that are thought to contribute both to the resting potassium conductance – the dominant resting ionic conductance in most neurons (see, e.g., Wright, [48]) – and to the conduction mediated by an important class of metabotropic, inhibitory synaptic receptors activated by  $\gamma$ -aminobutyric acid (the GABA<sub>B</sub> receptors) [49-52]. Because NMDA and non-NMDA (i.e.,  $\alpha$ -amino-3-hydroxy-5-methyl-4-isoxazolepropionic acid, or AMPA) glutamatergic receptors are often co-located in vertebrate cortical neurons, the implications with respect to other excitatory synaptic receptors are also considered. Secondary or dependent effects, such as those due to the opening of calcium- and voltage-dependent ion channels are not considered at present, with one important exception: the calcium-activated potassium (SK) channels that are also co-located with glutamatergic synapses in the dendritic spines of pyramidal neurons [53,54]. These channels, like Kir channels, are inward-rectifying [55,56], and they are activated by the calcium conducted into the spine by NMDAR channels. For brevity, I use the abbreviation *IRKC* to refer to inward-rectifying potassium channels including both Kir and SK types.

During the course of analysis, I examine a single electrical compartment, and then a neural process (a cable-like dendrite). In analyzing the latter, I apply mathematical results obtained by Gutman and co-workers for dendritic bistability arising from slow inward calcium currents [57,58].

## 1 Methods

Neurons were modeled to first order as single electrical compartments, and subsequently as a single-compartment soma coupled electrically to cable-like dendrites. Analysis of stationary versions of the governing equations, which include the instantaneous effects of synaptically-mediated conductances as well as other ion channels, was performed. The equations were normalized with respect to conductances or resistances and the electrical lengths of the dendrites, although not with respect to membrane potential since its characteristic values are familiar to physiologists.

Numerical analysis was performed primarily with SPICE (Simulation Program with Integrated Circuit Emphasis), a tool that is intended for electronic circuit simulations and is optimized for solution of stiff nonlinear equations. SPICE can solve static equations to obtain dc/equilibrium states. Discrete elements are described by electrical constitutive relations involving their interconnection points or nodes, and governing equations for interconnected circuits are automatically generated by application of Kirchhoff's current law (conservation of charge). Built-in linear elements or user-definable nonlinear voltage-controlled current sources were used for the implementation of various membrane conductances. The product T-SPICE (Tanner Research, Monrovia, CA) was used for the study. In addition, MATLAB (MathWorks, Natick, MA) and Excel (Microsoft, Redmond, WA) were used for supporting analysis.

### 1.1 Models for Membrane Conductance

The macroscopic electrical characteristics of ion channels (i.e., the mean electrical properties of some large number of such channels) were modeled with equations giving

current as a function of membrane potential. Conceptually, the function for each class of channel was separated into two factors: a *conductance parameter* and a canonical *voltage-dependent function* with dimensions of volts. Each voltage-dependent function is zero at a unique value of the membrane potential corresponding to the channel *reversal potential*, and (except for the NMDA model) was written in a form in which the reversal potential appears as a parameter. The conductance parameter is supposed to account for average conductance and total number or density of conducting channels; for synaptically-mediated conductances, it is proportional to the degree of synaptic activation. By convention, the conductance parameter was equated to the slope of the current-voltage relationship *at the reversal potential*, and accordingly, the canonical voltage-dependent functions were scaled to unity slope at their reversal potentials. For nonlinear I-V relationships, this convention allows the unambiguous expression of *relative conductance* as the ratio of conductance parameters as defined above (although this ratio may not correspond to empirical values obtained from local conductance measurements, if the nonlinearity is significant). In analyzing the dependence of neural dynamical regimes on synaptically-mediated channels, their instantaneous conductance was typically specified relative to resting membrane conductance.

### 1.1.1 Channel Models

Following I derive expressions for the canonical voltage-dependent function characterizing each class of channel model considered. In addition to NMDARs, these included an ohmic model, a model based on the *Goldman-Hodgkin-Katz* (GHK) equations [59,60], and a model for inward-rectifying potassium channels. Although the ohmic model is often employed in computational neurobiology [61], in reality it is usually an approximation to the more physiologically realistic GHK equations. IRKCs are not described well by either model; their conductance falls off rapidly with increasing membrane potential for outward currents (i.e., at membrane potentials above the potassium reversal potential). Although the particular model used herein is based on empirical characteristics of Kir channels, it also captures the most significant conductive characteristic that they have in common with SK channels – the inward-rectifying nonlinearity – and thus will be regarded as at least generally representative of SK channels as well.

The macroscopic electrical properties of NMDARs were modeled with an expression derived by Jahr and Stevens [2] in which the mean current-voltage relationship in a patch of membrane takes the form

$$I_{NMDA} = \frac{G_{nb}V_m}{1 + a[Mg^{2+}]exp(-kV_m)}, \quad (1)$$

where  $I_{NMDA}$  is the current,  $G_{nb}$  the macroscopic NMDAR conductance in the absence of magnesium blockade that gives rise to nonmonotonic behavior,  $V_m$  is membrane potential, and  $[Mg^{2+}]$  the extracellular magnesium concentration. The constants  $a$  and  $k$  were assigned the values estimated by Jahr and Stevens,  $0.28\text{mM}^{-1}$  and  $62\text{V}^{-1}$  respectively, unless otherwise indicated. A value of  $[Mg^{2+}] = 1.2\text{mM}$  was also assumed, so that  $b \equiv a \cdot [Mg^{2+}] = 0.336$ . With this definition, the canonical voltage-dependent function derived from the Jahr-Stevens model can be written

$$f_N(V_m) = \frac{(1+b)V_m}{1+b \exp(-kV_m)}. \quad (2)$$

The reversal potential associated with this model is 0V and is omitted as a parameter.

It is important to note that the channel conductance parameter used in conjunction with this model reflects the slope of the I-V relation under nearly unblocked conditions, and this must be kept in mind when considering conductance ratios or comparing currents with those of other ion channels – particularly when measured near the resting potential, where magnesium blockade is pronounced. For example, in the case of co-located glutamatergic receptors in rat pyramidal neurons, Watt et al. [62] estimate that the ratio of NMDAR to AMPA receptor currents is on the order of 0.4 in miniature excitatory post-synaptic currents. Numerical analysis shows that, at a membrane potential  $V_m = -70\text{mV}$ , the NMDAR conductance parameter multiplying the function in (4) would have to be 8 *times larger* than AMPA conductance to produce currents in that ratio. (In this analysis, AMPA conductance was treated as ohmic with  $V_{r0} = 0\text{V}$ .) This is a straightforward consequence of the profound nonlinearity of the NMDAR I-V relation.

For ohmic ion channels, the voltage dependent form is simply

$$f_O(V_m; V_{r0}) = V_m - V_{r0}. \quad (3)$$

For channels modeled with the Goldman current equation [59,60], the function was derived from the expression for membrane current flux  $i_C$  carried by a univalent cation  $C$ :

$$i_C \propto \frac{V_m \{ \exp(V_m/V_T) [C]_{in} - [C]_{out} \}}{\exp(V_m/V_T) - 1}, \quad (4)$$

where  $[C]_{in}$  is the internal concentration of  $C$  and  $[C]_{out}$  its external concentration; and  $V_T$  is the thermal voltage  $RT/F$ , where  $R$  is the ideal gas constant,  $T$  absolute temperature, and  $F$  Faraday's constant. By applying the Nernst equation  $V_{r0} = V_T \ln([C]_{out}/[C]_{in})$  to introduce the reversal potential for  $C$ , and setting the slope of the I-V relationship to unity at  $V_{r0}$ , the canonical voltage-dependent function may ultimately be written

$$f_G(V_m; V_{r0}) = \frac{V_T V_m \{ \exp(V_{r0}/V_T) - 1 \} \{ \exp(V_m/V_T) - \exp(V_{r0}/V_T) \}}{V_{r0} \exp(V_{r0}/V_T) \{ \exp(V_m/V_T) - 1 \}}. \quad (5)$$

A similar exercise yields the same result for a univalent anion. The Goldman current dependence reduces to ohmic at  $V_{r0} = 0$  (i.e., when internal and external concentrations in (4) are equal).

Finally, the characteristics of IRKCs were modeled by hand-fitting an *ad hoc* function to data obtained by Sodickson and Bean [50] for Kir channels in rat CA3 hippocampal neurons. The canonical voltage-dependent form for this channel class is

$$f_{Kir}(V_m; V_{r0}) = \frac{d \{ \tanh[(V_m - V_{r0} - c)/d] - e \}}{1 - \tanh^2(c/d)}, \quad (6)$$

where  $\tanh$  denotes hyperbolic tangent,  $d$  was assigned the value 25mV and  $e$  the value 0.5 based on the hand fit, and  $c$  took the value  $-13.73\text{mV}$  in order to place the zero-crossing of the function at  $V_m = V_{r0}$ . In practice,  $V_{r0}$  is the only free parameter and is

identified with the reversal potential for potassium  $V_{rK}$ . The fit to Sodickson and Bean's empirical data, with  $V_{r0} = -92\text{mV}$  and the expression for  $f_{Kir}$  above multiplied by the conductance parameter  $4.4\text{nA/V}$ , is shown in Fig. 1.

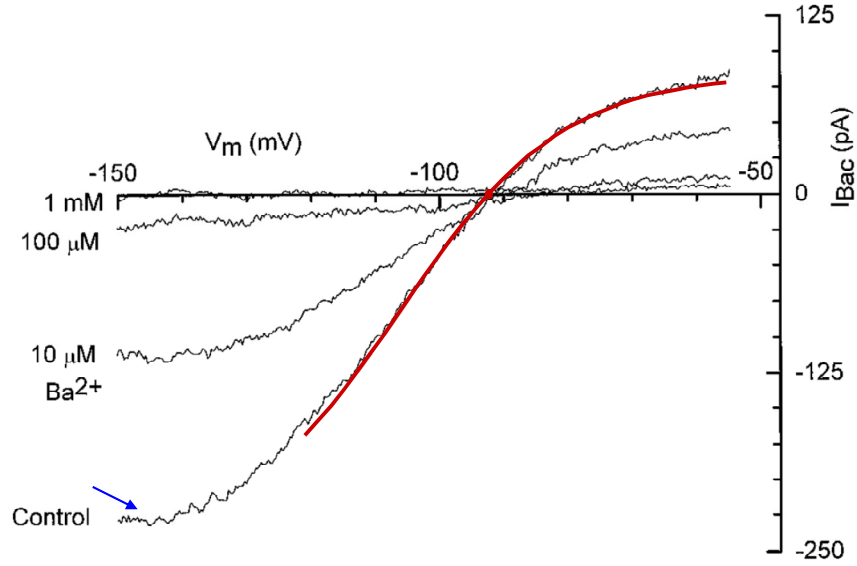


**Fig. 1.** Fit of an *ad hoc* canonical voltage-dependent function (in red) to experimental data for the voltage dependence of Kir channel current in rat CA3 hippocampal neurons. The fit for these data is obtained by setting the reversal potential  $V_{r0}$  to the experimentally-observed value of  $-92\text{mV}$ , and multiplying the function  $f_{Kir}$  in Equation (6) by the conductance parameter  $4.4\text{nA/V}$ . The data represent the Kir I-V relation in a control case under physiological conditions (i.e., without added  $\text{Ba}^{2+}$ ), and are reproduced with permission from Sodickson and Bean (1996).

## Resting Membrane Model

The resting potential in neurons is primarily due to membrane potassium conductance, but smaller chloride and sodium conductances also contribute (see, e.g., Wright [48]). When NMDARs are activated in conjunction with the resting conductance alone, the sum influence of these other channels determines the dynamical regimes possible. For purposes of illustration, a particular, physiologically plausible resting membrane model was constructed and used in simulations of compartments and dendrites. Parallel chloride and sodium conductances were set to 30% and 4.9% of the total potassium conductance, respectively, and represented by the Goldman model. Potassium conductance was evenly split between Goldman and Kir models (the former representing non-rectifying ‘leakage’ conductance). The complete model was cast in the canonical form, as the product of a conductance parameter  $G_R$  and a voltage-dependent function  $f_R(V_m)$ :

$$f_R(V_m) = \alpha [0.5 f_{Kir}(V_m; V_{rK}) + 0.5 f_G(V_m; V_{rK}) + 0.3 f_G(V_m; V_{rCl}) + 0.049 f_G(V_m; V_{rNa})] \quad (7)$$

Chloride and sodium reversal potentials  $V_{rCl}$  and  $V_{rNa}$  were set to  $-70\text{mV}$  and  $+60\text{mV}$ , respectively, and the potassium reversal potential  $V_{rK}$  to  $-85\text{mV}$ , resulting in a resting potential of  $-70\text{mV}$ . The constant  $\alpha$  assumed the value  $0.751$  in order to achieve unity slope at the resting potential.

## 1.2 Neural Models

In equivalent circuits for a neuron or neural process, the potential of the extracellular space was regarded as the reference potential (ground). Channel models were configured so as to conduct current from the intracellular space to an ideal voltage source defined with respect to ground, and representing the reversal potential associated with the particular class of channel. Positive current by convention corresponds to (positive) charge flowing out of a neuron.

### 1.2.1 Single Compartment Models

For single-compartment models involving NMDAR and one other class of ion channel, the complete membrane I-V relation is written in the form

$$I_m = G_N f_N(V_m) + G_0 f_0(V_m; V_{r0}) + C_m dV_m / dt, \quad (8)$$

where  $I_m$  is the membrane current,  $V_m$  the membrane potential, the functions  $f_N(V_m)$  and  $f_0(V_m; V_{r0})$  are canonical expressions for the voltage dependence of the NMDA and non-NMDA channels, respectively,  $G_N$  and  $G_0$  are their respective conductance parameters, and  $C_m$  is membrane capacitance. For stationary analyses, the  $dV_m/dt$  term is dropped, and normalization with respect to conductance is accomplished by dividing by  $G_0$ :

$$I_m / G_0 = \Gamma f_N(V_m) + f_0(V_m; V_{r0}), \quad (9)$$

where  $\Gamma$  is the ratio of the NMDA to non-NMDA conductance  $G_N/G_0$ .

In some single-compartment simulations, membrane conductance included the resting model in parallel with NMDAR and additional IRKC conductance. The latter were intended to be representative of either open Kir channels associated with GABA<sub>B</sub> receptors, or SK channels, and were modeled with the Kir voltage dependence in (6). The magnitude of the additional Kir conductance was specified relative to the resting conductance by a parameter  $K$ , and NMDAR conductance was also specified relative to resting conductance by a parameter  $N$ . In this case, the governing stationary equation may be written

$$I_m / G_R = N f_N(V_m) + K f_{Kir}(V_m; V_{rK}) + f_R(V_m). \quad (10)$$

### 1.2.2 Dendritic Models

Long, thin dendrites are often modeled with one-dimensional cable equations (see, e.g., Rall [63]), with membrane current paths approximated as continuous conductances per unit length of dendrite. For concreteness and to limit the degrees of freedom in the analyses described herein, membrane conductance in all dendrites was assumed to include the resting conductance modeled by (7) in parallel with active NMDAR and IRKCs. The full cable equation in this case may be written

$$\frac{\partial^2 V_m}{\partial x^2} = r_a \left( \nu g_R f_N(V_m) + \kappa g_R f_{Kir}(V_m; V_{rK}) + g_R f_R(V_m) + c_m \frac{\partial V_m}{\partial t} \right), \quad (11)$$

where  $x$  is axial position along the dendrite,  $r_a$  is axial resistance (assumed ohmic) per unit length,  $g_R$  is the specific resting membrane conductance parameter per unit length, and  $c_m$  is membrane capacitance per unit length. The parameter  $\nu$  is the local ratio of NMDAR to rest conductance per unit length and  $\kappa$  the local ratio of additional Kir to rest conductance per unit length, analogous to  $N$  and  $K$  in (10). Membrane potential  $V_m$  is implicitly dependent on axial position  $x$ . Axial current at any point in the dendrite is equal to  $-(1/r_a)\partial V_m/\partial x$ . As in the single compartment, the  $\partial V_m / \partial t$  term is dropped from (11) for stationary analysis.

Boundary conditions imposed on a dendrite determine the form of particular solutions (i.e.,  $V_m$  as a function of  $x$ ) to the stationary version of (11). At the proximal end ( $x = 0$  by convention), this boundary condition is associated with the termination of the dendrite on a soma or another segment of neural process. The dendritic current at the proximal termination,  $-(1/r_a)dV_m/dx|_{x=0}$ , can be regarded as the output of the dendrite as a whole. By the convention adopted above, it is positive when positive charge flows into the dendrite.

For purposes of the analyses herein, the electrical properties of any dendritic segments under consideration were assumed to be uniform along the length. In such case, non-dimensionalization of the stationary version of (11) with respect to length and resting conductance can be achieved by dividing by  $r_a$  and  $g_R$ , yielding

$$\frac{\partial^2 V_m}{\partial \chi^2} = \nu f_N(V_m) + \kappa f_{Kir}(V_m; V_{rK}) + f_R(V_m), \quad (12)$$

where  $\chi$  is a non-dimensionalized axial coordinate  $\chi \equiv x/\lambda_R$ , where  $\lambda_R = (r_a g_R)^{-1/2}$  is a conventional *electrotonic length constant*, equal to the length at which the total axial resistance in the dendrite is equal to the inverse of the total parallel conductance of the resting membrane. This characteristic resistance value is  $R_R = (r_a/g_R)^{1/2}$ .

At this point, I consider some estimates of the absolute conductance and resistance parameters for an example biological dendrite, in order to form an idea of the dimensions of a realistic model and limits on its parameters. Values of  $100\Omega\text{cm}$  for cytoplasmic resistivity and  $25\mu\text{S}/\text{cm}^2$  for membrane specific conductivity are within the physiological range, and with an assumed diameter of  $0.5\mu\text{m}$ , this would give an axial resistance per unit length  $r_a$  of  $5.09\text{M}\Omega/\mu\text{m}$  and resting specific membrane conductance  $g_R$  of  $0.393\text{pS}/\mu\text{m}$ . Lazarewicz et al. [41] developed an estimate of NMDAR density on the dendrites of hippocampal pyramidal neurons based on estimates of receptor density [64,65] and conductance [66] such that at complete activation the specific NMDAR conductance is  $120\text{pS}/\mu\text{m}$ . This is about 305 times as large as the rest conductance computed above, providing an absolute upper bound on the parameter  $\nu$ , with much smaller values likely *in vivo*. For most simulations reported herein,  $\nu$  assumed values in a range about 20, and  $\kappa$  values in a range about 9; these values were selected as representing ‘moderate’ levels of channel activation, and they support a bistable membrane characteristic in conjunction with the resting membrane model. At  $\kappa = 9$ , the added Kir conductance is 24 times as large as the resting Kir conductance.

For numerical solution, dendrites were discretized into 100 electrical compartments. Each had its own lumped membrane conductance and axial resistance. Electrical lengths in all simulations were  $\leq 2.0\lambda_R$ . A Neumann boundary condition corresponding to a sealed end was implemented by leaving the distal axial terminal of the most distal compartment unconnected; Dirichlet (voltage-clamped) or Robin (finite proximal load) boundary conditions at the proximal termination were implemented by connecting the proximal axial terminal of the most proximal compartment to a voltage source or a model load, respectively.

### **1.3 Analysis of Instantaneous Dynamical Regimes**

Bistability and the conditions supporting it were characterized using the discretized versions of the stationary equations (9), (10) and (12). Characterization was accomplished in some cases by inspection of the stationary membrane current-voltage relationship for various values of relevant parameters, allowing identification of unstable as well as stable equilibria, and in some cases by solving for membrane voltage or postsynaptic current at various equilibrium states as a parameter of interest was varied up or down. Such sweeps typically transitioned from monostable through bistable regimes, and the locations of abrupt changes in the membrane potential corresponding to such transitions could be directly observed.

Incremental membrane resistance and gains in monostable regimes were characterized by numerical computation of the relevant derivatives. In addition, a measure of dendritic *current gain* was developed by considering the effects on the dendritic output current of an incremental test current injected across the dendritic membrane, uniformly distributed along its length. The NMDAR-induced current gain was defined as the ratio of the change in the output current with NMDAR activation present, to the change induced by the same test current in the passive dendrite.

## **2 Results**

### **2.1 Bistability and Amplification in an Electrical Compartment**

#### **2.1.1 Characteristic Dependence on NMDAR and Non-NMDAR Channels**

To give a broad idea of the joint dependence of the dynamical states of a neuron on the characteristics of NMDAR and other classes of ion channels, the function  $f_0(V_m; V_{r0})$  in equation (9) was identified in separate analyses with the voltage-dependent functions  $f_{ohmic}(V_m; V_{r0})$ ,  $f_G(V_m; V_{r0})$ , and  $f_{Kir}(V_m; V_{r0})$  defined for the ohmic, Goldman, and Kir models, respectively, in Section 1.1.1. Because only the NMDAR current has a nonmonotonic voltage dependence, with a single point of inflection, the total membrane current in such a compartment may have either one or three zeros but no more; these correspond respectively to the equilibria associated with monostable and bistable dynamical regimes.

Results for the NMDAR model in conjunction with the ohmic model are used here to illustrate the characteristics of these regimes. Depicted in Fig. 2 are computed I-V

relationships (corresponding to the results of voltage-clamp experiments with the voltage varied) for the compartment. Curves were generated for several values of the ratio  $\Gamma$  of NMDAR to non-NMDA conductance, and ohmic channel reversal potential  $V_{r0}$ . In Fig. 2a, for which  $V_{r0} = -90\text{mV}$ , curve *B* corresponds to a bistable compartment, while curve *A* corresponds to a 'boosting' regime and curve *C* to a 'self-triggering' regime as defined by Schiller and Schiller [30]. Also shown in Fig. 2b is an equilibrium manifold for this  $V_{r0}$ , including the membrane potentials corresponding to both stable and unstable equilibria, and indicating the *limit points* of each stable branch of the curve. In the terminology of dynamical systems theory, these correspond to co-dimension one *saddle-node* or *fold bifurcations* [41,67,68] at which the system transitions between one and three equilibrium states. Abrupt quasistatic transitions can occur between the stable branches at the limit points, in the directions indicated by the dashed arrows. A fourth regime exists in the parameter space, in which bistability is not evoked for any value of  $\Gamma$ ; an example is characterized by the I-V curves in Fig. 2c, in which  $V_{r0}$  took the value  $-70\text{mV}$ . I refer to such a regime as  $\Gamma$ -*monostable*, indicating that monostability prevails for any value of NMDAR conductance relative to other membrane conductances. The curve in Fig. 2d represents (in a sense) a boundary between the first three regimes and the fourth; it corresponds to a *cusp bifurcation* as detailed below.

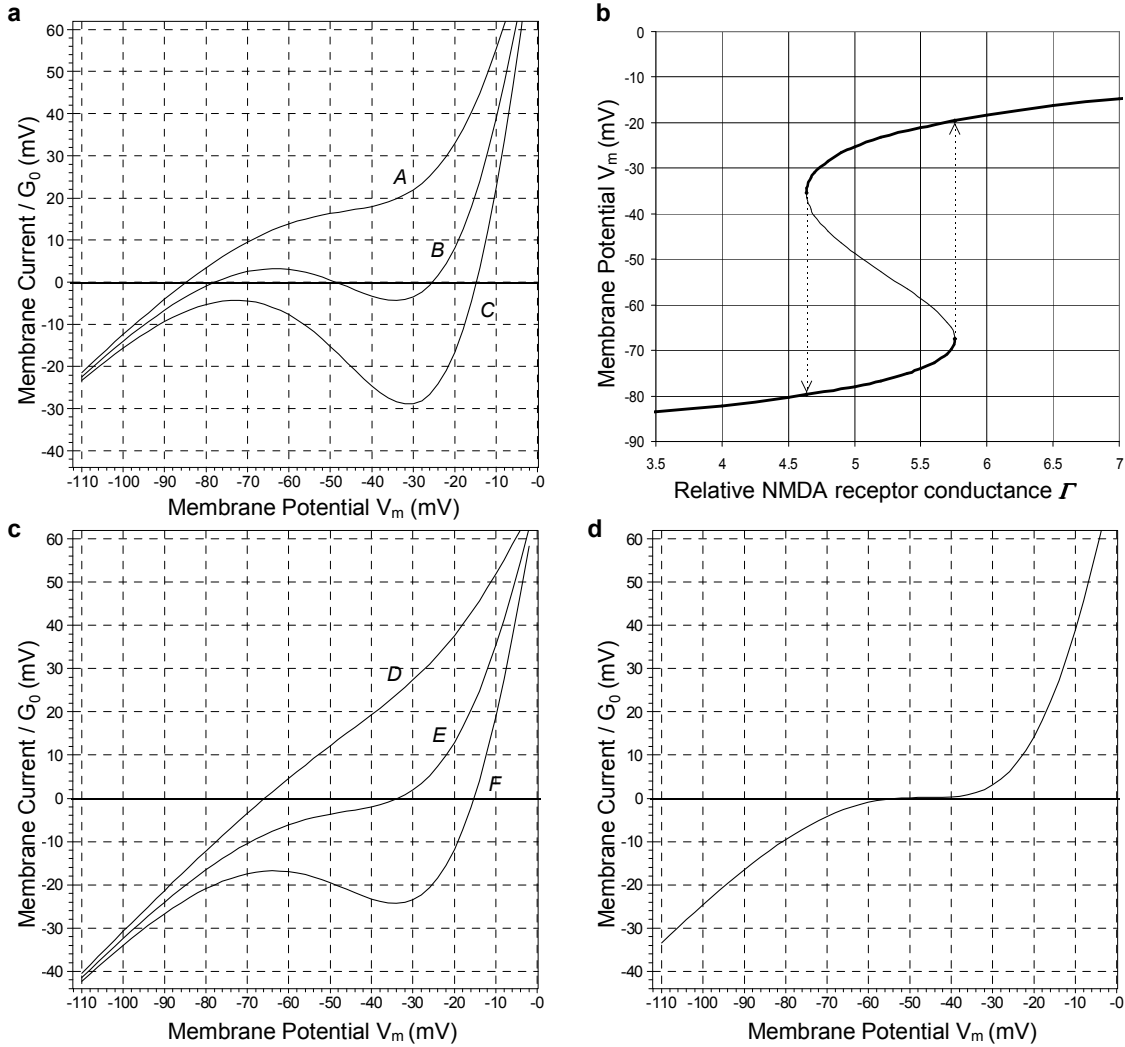


**Fig. 2.** Membrane I-V relationships and dynamical states of a single electrical compartment. The membrane contains both NMDAR and ohmic conductances. The NMDAR conductance parameter is expressed by its ratio  $\Gamma$  to the ohmic conductance. Panel *a* depicts the membrane current (normalized by the ohmic conductance) as a function of membrane potential, for *A*)  $\Gamma = 3$ ; *B*)  $\Gamma = 5$ ; *C*)  $\Gamma = 7$ ; with ohmic reversal potential  $V_{r0} = -90\text{mV}$ . The compartment is monostable for curves *A* and *C* and bistable for curve *B*. Panel *b* depicts the equilibrium manifold for this system, i.e., the possible equilibrium potentials as a function of  $\Gamma$  with  $V_{r0} = -90\text{mV}$ . Heavy curves indicate stable equilibria and the light curve, unstable equilibria. Dashed lines indicate possible transitions between the stable branches at the *limit points* of the stable equilibria, in the directions indicated by the arrows, and define a *hysteresis loop*. Panel *c* depicts membrane current as a function of membrane potential, for *D*)  $\Gamma = 1$ ; *E*)  $\Gamma = 3$ ; *F*)  $\Gamma = 5$ ; with ohmic reversal potential  $V_{r0} = -70\text{mV}$ . The compartment is monostable in all cases. Panel *d* depicts membrane current as a function of membrane potential for  $\Gamma = 3.56$  and  $V_{r0} = -78.2\text{mV}$ , and corresponds to a *cusp bifurcation* as detailed in the text.

Fig. 3 depicts these regimes in the space spanned by the parameters  $\Gamma$  and  $V_{r0}$ , for the Goldman, ohmic, and Kir models in conjunction with NMDAR conductance. The bistable region in each case is bounded by a pair of curves that converge at a point on the right. A 'boosting' regime lies below each pair of curves, and a 'self-triggering' regime above. The point of convergence corresponds to a co-dimension two cusp bifurcation, at

which two saddle nodes meet and annihilate each other [41,67,68]. The system is  $\Gamma$ -monostable for non-NMDA reversal potentials more positive than the value at the cusp. As the voltage dependence of the current in the non-NMDA model varies from superlinear (the Goldman model) to linear to sublinear (the Kir model) in character, the point of the cusp moves to more positive potentials, and the bistable region expands in size. This dependence is of physiological significance: it indicates, for example, that a class of ion channel that obeys the GHK equations is capable of inducing bistability in conjunction with NMDAR channels only if its reversal potential is strongly hyperpolarizing. The resting membrane potential in most neurons is higher than the values at the cusps in Fig. 3, except for the Kir + NMDAR combination, and indeed, the example resting membrane model constructed in Section 0 results in a  $\Gamma$ -monostable compartment in concert with the NMDAR channel model.

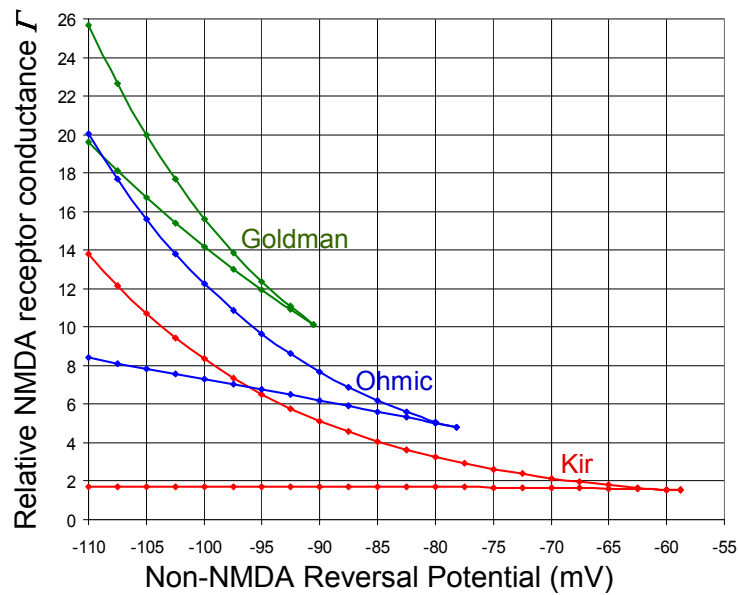


**Fig. 3.** Bistable regions of a single electrical compartment. Regions are depicted in the space spanned by the ratio  $\Gamma$  of NMDAR to non-NMDA conductance and the reversal potential  $V_{r0}$  of the non-NMDA conductance, for three models for the non-NMDA conductance, Goldman, ohmic, and Kir models, as indicated.

However, the true values of the parameters characterizing NMDARs *in vivo* are not precisely known, and in addition there are several different receptor subtypes [69] (more than one of which may be expressed within the same phenotype) that would be expected to have differing electrical characteristics. In the NMDA model used to produce Fig. 3 the parameters estimated by Jahr and Stevens [2] were employed, with the model parameter  $k$  set to  $62 \text{ V}^{-1}$ , but this parameter has assumed values as large as  $80 \text{ V}^{-1}$  in modeling studies in the literature [70]. Larger values move the location of the cusp bifurcation to more positive potentials, i.e., expand the region of bistability. For example, for the ohmic model the cusp occurs at  $V_{r0} = -78.2 \text{ mV}$  when  $k = 62 \text{ V}^{-1}$ , but moves to  $V_{r0} = -60.5 \text{ mV}$  when  $k$  is set to  $80 \text{ V}^{-1}$ . Similarly, the resting membrane model of Section 0 supports a bistable regime at the higher value of  $k$ , although for a limited range of  $\Gamma$  values.

### 2.1.2 Facilitation and Amplification

In addition to bistability, *amplification* is another computationally significant effect that can be mediated by NMDARs in conjunction with other conductances. As NMDARs are progressively activated in a  $\Gamma$ -monostable regime, the membrane potential as a function of  $\Gamma$  reaches and passes through a region of relatively rapid depolarization. This nonlinearity can be exploited to achieve coactivation-dependent facilitation, in which there is a superlinear response to the number or density of NMDA synapses activated. However, it can also be regarded as setting up an amplifying state, in which current injected by other classes of synaptic receptors has a greater effect on membrane potential than it would in the resting state. This is reflected by an increased *incremental membrane resistance* in the high-slope regime. This mode of action is particularly significant given the co-location of NMDA and non-NMDA excitatory glutamatergic receptors within the dendritic trees of CNS neurons – in fact, in pyramidal cells, at the same synapses [53,54,71]. Fig. 4a (blue trace) depicts membrane potential of a single compartment as a function of relative NMDAR conductance for the NMDAR model in parallel with the resting membrane model, and Fig. 4b (blue trace) shows the corresponding incremental membrane resistance relative to the rest state (i.e., multiplied by the rest conductance).

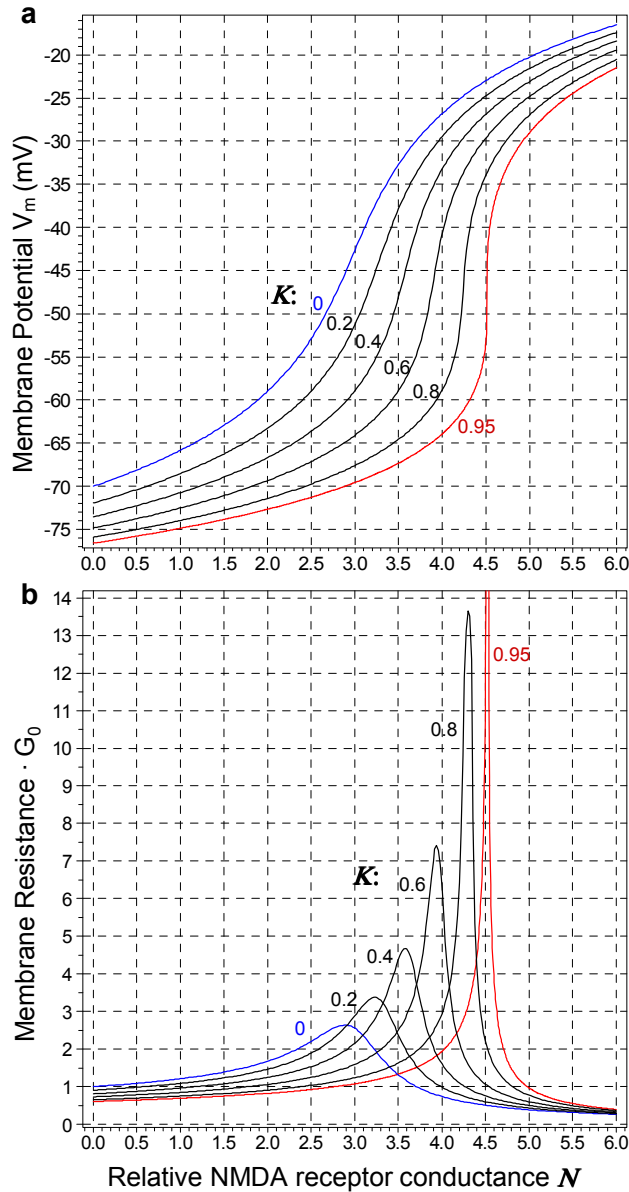


**Fig. 4.** Membrane potential and incremental membrane resistance in a single electrical compartment. Each is depicted as a function of  $N$ , the ratio of NMDAR to resting conductance. The model contains additional Kir conductance beyond that in the resting membrane, parameterized by its ratio  $K$  to the rest conductance, and meant to represent the effects of activated Kir or SK channels. Membrane potential is shown in Panel a, and incremental membrane resistance, normalized by multiplication by the rest conductance, in Panel b. The blue curves are for NMDARs in conjunction with rest conductance alone; the compartment is monostable for the blue and black curves, while the red curves correspond to a cusp bifurcation.

## The Role of Inward-Rectifying Potassium Channels

With regard to NMDAR-induced bistability and amplification, it is clear that potassium conductance also plays a significant role; increasing the relative magnitude of any of the other ion channel conductances considered would push the cusp bifurcation of the system to more negative values of the compartment equilibrium potential. The results

for the Kir model demonstrate that increasing IRKC conductance has the reverse effect – and for this reason, the co-location of either GABA<sub>B</sub> synaptic receptors or active SK channels with NMDARs in a neuron is a subject of particular interest. As expected, simulations of a compartment with parallel resting and active conductances demonstrate that an increase in inward-rectifying potassium conductance can induce bistability in an otherwise monostable compartment, and then expand the range of NMDAR activation over which bistability prevails.

Such an increase also affects the amplifying characteristics of a compartment when in a  $\Gamma$ -monostable regime. In addition to the case of NMDARs acting in concert with rest conductance alone ( $K = 0$ ), Fig. 4 depicts how the dependence of membrane potential and incremental membrane resistance on NMDAR activation (i.e.,  $N$ ) varies with IRKC activation (parameterized by  $K$ ). For the black traces in Fig. 4, the system is  $\Gamma$ -monostable; the red traces depict membrane potential and incremental resistance as the system reaches a cusp bifurcation, which occurs at  $K = 0.95$ . As  $K$  increases, the effect is inhibitory in the sense that the compartment hyperpolarizes for low levels of NMDAR activation, and the steep part of relation between  $V_m$  and  $N$  is pushed to higher values of  $N$ . However, in the vicinity of that steep region, the gain with respect to injected currents (as quantified by the membrane resistance) dramatically *increases* with IRKC activation, and the system is capable of powerful amplification of small changes in input, whether these occur at NMDA or other classes of synapses. This effect is due simply to the interaction between the nonlinearities of the NMDAR and IRKC I-V relations. A limit is reached at the cusp bifurcation, where the membrane resistance becomes infinite as a discontinuity appears in the relationship between  $V_m$  and  $N$ .

Coactivation of GABA<sub>B</sub> synapses or SK channels with NMDARs thus provides a potentially powerful computational mechanism for facilitation, amplification, and short-term memory functions. SK channels are found in intimate association with glutamatergic synapses in dendritic spines, and are (in a sense) automatically activated, at least in part by calcium influx through NMDARs themselves. GABA<sub>B</sub> synapses, conversely, provide a mechanism for *independent* control of facilitation and amplification. Pharmacological evidence suggests that, like NMDARs, GABA<sub>B</sub> receptors are distributed in the dendritic trees of CNS neurons in which they occur [72].

## **2.2 Bistability and Amplification in a Neural Process**

### **2.2.1 Characteristics of Dendritic Bistability and Amplification**

Consider next the dynamical regimes of a neural process, i.e., a *dendrite*, modeled by the stationary equation (12). When the membrane current per unit area is a nonmonotonic function of membrane potential  $V_m$ , there is potential for bistable behavior; the axial resistance as well as membrane properties may play a role in inducing such behavior. By varying the relative magnitudes of the active conductances in (12) over physiologically reasonable ranges, a variety of membrane I-V characteristics can be generated, including monotonic, nonmonotonic (N-shaped) with a single zero, and nonmonotonic with three zeros. Although this paper is concerned with NMDARs, many of the results discussed below are relevant whenever a nonmonotonic membrane I-V characteristic prevails. The

resultant dynamical regimes are rather more complicated in a dendrite than a single compartment.

The theory of the bistable dendrite has been advanced to a considerable degree by Gutman and coworkers [57,58,73,74]. The dendritic model they considered also comprised a one-dimensional cable equation with spatially uniform conductive properties, and with a *bistable membrane I-V characteristic*. The physiological basis of this was the presence of slow, persistent inward calcium currents, but the theory can be applied equally well to bistability associated with NMDAR channels.

Gutman [57,58] considered the stationary boundary-value problem in which the dendrite is sealed (i.e., allows no current flow) at the distal end (resulting in a Neumann boundary condition), and is voltage-clamped at the proximal end (a Dirichlet boundary condition). Several important theoretical results obtained for this model [57] can be summarized as follows:

1. Below a critical dendritic length, the solution  $V_m(\chi)$  of the stationary equation is unique for all values of the proximal clamp voltage, and the relationship between the current flowing into the dendrite and the clamp voltage is single-valued;
2. For dendrites longer than this critical length, the solution is *not* unique for some range of values of the clamp voltage. The current flowing into the dendrite may assume any of two or more values for any clamp voltage within this range. Furthermore, this voltage range increases as the length of the dendrite increases;
3. The *number* of possible solutions within this voltage range also increases as dendritic length increases, but all except two of these solutions are unstable. The stable solutions each feature a monotonic dependence of  $V_m$  on  $\chi$ , with the potential at the distal end approaching either the largest or smallest zero-crossing voltage of the membrane I-V relation. There are thus two possible *stable* values of current into the dendrite for any clamp voltage within the range. For brevity, I refer to such pairs of stable solutions as, respectively, the *high* and *low states*.

To illustrate the character of these solutions for a dendrite with active NMDARs, Fig. 5a depicts simulation results for current flowing into a dendrite as a function of the clamp voltage for the model (12), for parameter values  $\nu = 20$  and  $\kappa = 9$ , and with dendritic length  $A$  in non-dimensionalized coordinates as a parameter. Fig. 5b shows examples of the membrane potential in the dendrite as a function of  $\chi$ , for a dendrite long enough to support bistability. The clamp voltage is a parameter.

Gutman and coworkers [57,75] defined dendritic bistability in the narrow sense described above: as the existence of two possible stable states, with two different currents into the dendrite, when the process is voltage-clamped proximally. I refer to this as *Dirichlet bistability*. The voltage-clamp condition is not entirely relevant to *in vivo* physiology, but can be regarded as defining the stationary current-voltage relation for the dendrite *as a whole*, and from this point of view Dirichlet bistability is an intrinsic property of a dendrite, which in the present case is dependent on its instantaneous state of NMDAR and IRKC activation.

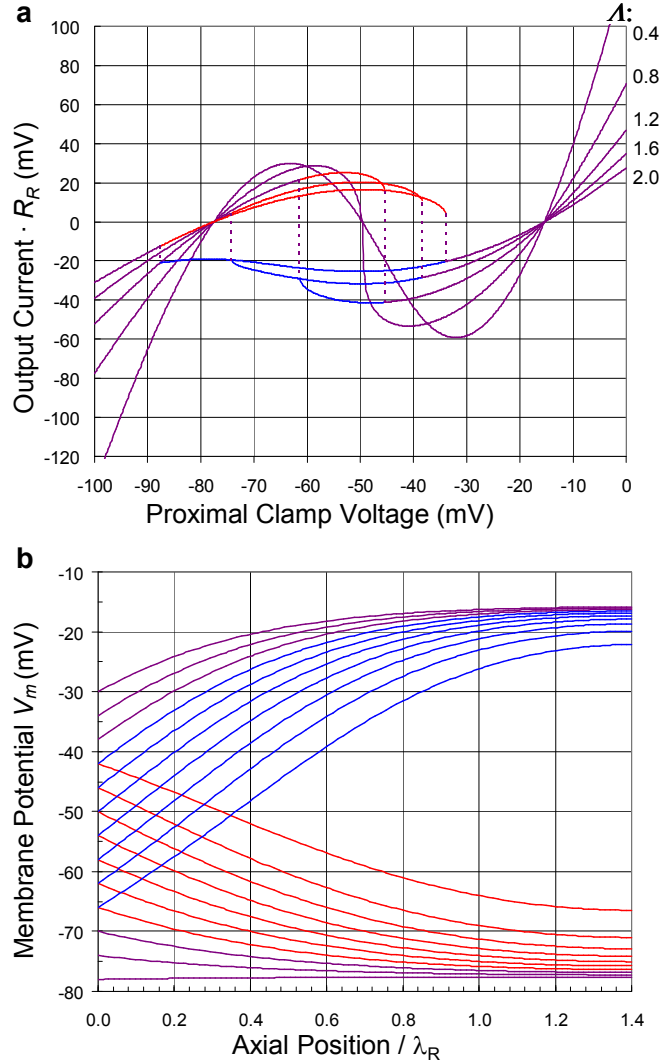


**Fig. 5.** Output characteristics of a dendrite with active NMDARs under a proximal Dirichlet boundary condition. Panel *a* depicts the dendritic output current (normalized by multiplying by the characteristic resistance  $R_R$  of a dendrite of unity electrotonic length) as a function of the clamp voltage defining the proximal boundary condition. Electrotonic length  $A$  of the dendrite is a parameter, taking the values indicated. Purple curves correspond to monostable regimes; blue curves indicate the high state and red the low state, in bistable regimes. Panel *b* shows possible distributions of membrane potential as a function of axial position in a dendrite with length ( $A = 1.4$ ) long enough to support bistability. The parameter is the proximal clamp voltage, which takes the value of the membrane potential at the y-intercept of each curve or pair of curves. Again monostable solutions are indicated by purple curves and bistable solutions by blue (the high state) and red (the low state) curves.

For given conductance parameters, the critical length at which Dirichlet bistability appears may be approximated [74]:

$$A_{crit} \cong (\pi/2)(-g_{min}/g_R)^{-1/2}, \quad (13)$$

where  $g_{min}$  is the minimum value of the slope of the (nonmonotonic) dendritic membrane I-V relation per unit length, and  $g_R$  the specific resting membrane conductance parameter. When expressed in absolute units, the critical length  $L_{crit} = \lambda_R \cdot A_{crit} \approx (\pi/2)(-g_{min}r_a)^{-1/2}$  is

independent of the choice of the rest state as reference, as expected from physical considerations. The quantity  $g_{min}/g_R$  corresponds to the minimum value of  $d/dV_m[vf_N(V_m) + \kappa f_{Kir}(V_m; V_{rK}) + f_R(V_m)]$ .

I examined Dirichlet bistability in dendrites with active NMDAR and inward-rectifying potassium conductance using (12) in conjunction with a sealed-end distal boundary condition. The expression in (13) was found to give good agreement with critical lengths obtained by numerical solutions of (12), so long as a bistable membrane I-V characteristic was present. Interestingly, however, I found that Dirichlet bistability can occur even when the membrane I-V relationship has only a single zero, so long as that relationship is nonmonotonic. Under these conditions, the two possible values of the output current are of the same sign. I refer to this phenomenon as *load-induced bistability*, which can be seen to arise due to the presence of axial resistance in the structure and current flow induced by the proximal clamp. Dirichlet bistability, whether load-induced or not, is associated with the emergence in some distal portion of the dendrite of a regime in which the relationship between an injected current and the local membrane potential is N-shaped with three zeros. Load-induced bistability can occur with activation of NMDARs only (i.e., with  $\kappa = 0$  in (12)), but because the axial resistance is ohmic, bistable regimes exist only for hyperpolarized proximal voltages (with the NMDAR model used in this study). This behavior mirrors that of the single compartment with parallel NMDAR and ohmic membrane conductance, in which bistable regimes exist only for ohmic reversal potentials below typical resting potentials.

In the context of a dendrite that is part of a neuron, the voltage-clamp boundary condition corresponds to an assumption that the dendrite has essentially no electrical influence on the soma and/or remainder of the neuron. Realistically, however, the remainder of a neuron must present a finite conductance (referred to hereafter as the ‘proximal load’), which may be large compared to the dendritic conductance if the dendrite terminates on or near the soma, or may be of similar magnitude if a length of passive neural process intervenes. Generally, as the conductance of this load becomes smaller (assuming it is passive in nature), the critical length for dendritic bistability correspondingly becomes smaller for a given density of active synapses. In any such case, the relevant boundary-value problem is determined by the condition that the current into the dendrite must match the current flowing out of the load. This results in a Robin-type boundary condition in which both the membrane potential and its spatial derivative appear. Via this boundary condition, the dynamical state of the dendrite is affected by the conductance *and* instantaneous reversal potential of the proximal load. (This reversal potential is, by definition, the value of the potential at the boundary for which no current flows from the remainder of the neuron.) The overall current-voltage relation for the dendrite alone, derived from the voltage-clamp analysis, is still conceptually useful in such cases: the dendrite may be regarded as an electrical ‘black box’ in parallel with the load conductance, and when the I-V relationship of the two taken together has three zeros, the dendrite is bistable in combination with the load.

A set of examples is shown in Fig. 6, in which this technique has been used to visualize the variety of regimes that can prevail in a dendrite governed by (12) in conjunction with a proximal Robin boundary condition. Parameters were chosen so that the dendritic membrane I-V relationship was nonmonotonic in each case, and the I-V relationship of the proximal load was linearized about its instantaneous reversal potential

*Eprox.* Fig. 6 shows by an exhaustive set of examples that dynamical regimes exist for this system with or without a bistable membrane I-V relation, with or without Dirichlet bistability, and with or without overall bistability of dendrite and load, in any possible combination. Each panel in Fig. 6 depicts the membrane I-V characteristic, the I-V relationship of the dendrite under Dirichlet boundary conditions, and the overall I-V relationship of the dendrite and load.

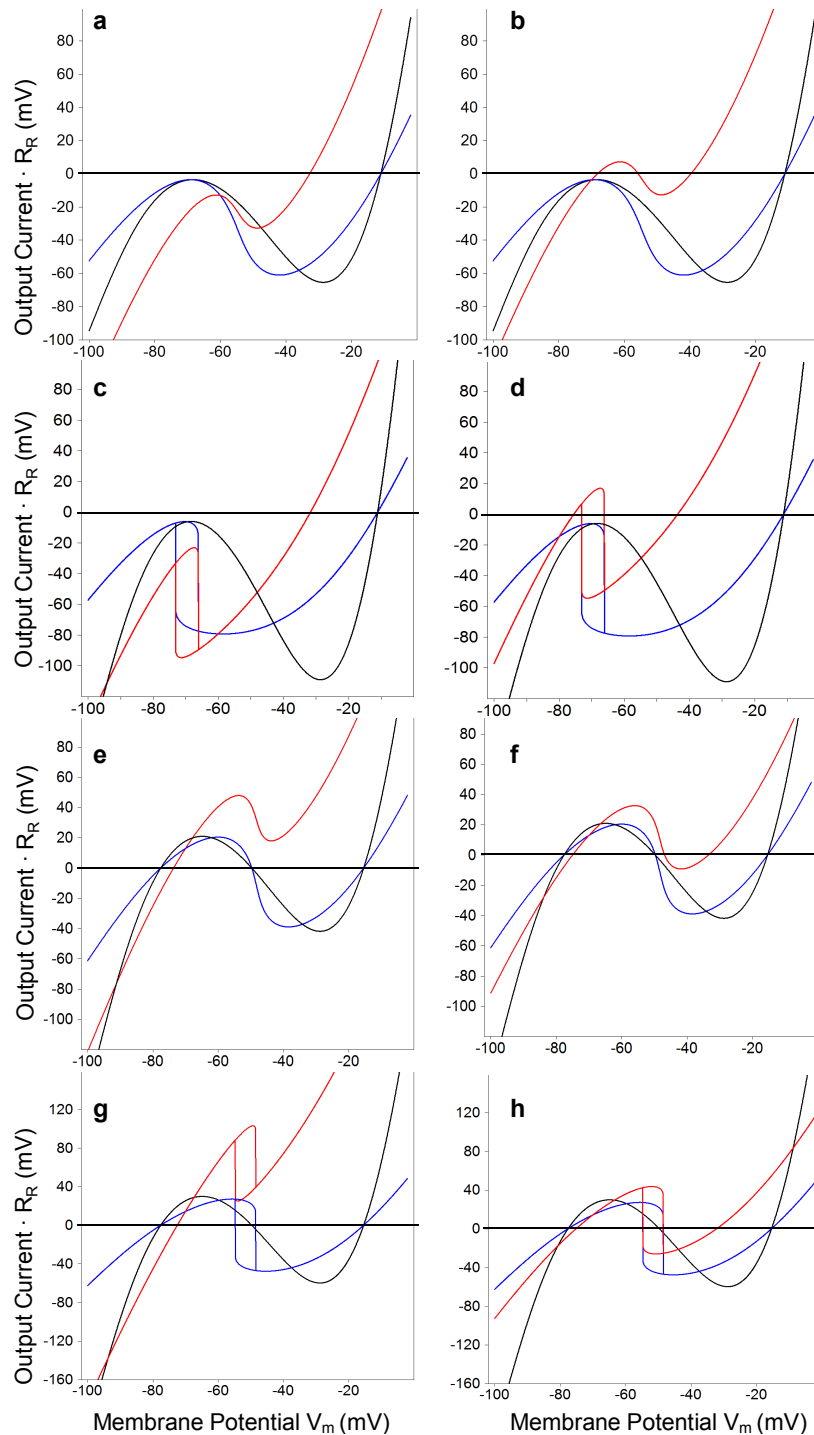


**Fig. 6.** Dendritic I-V relations and dynamical regimes. In all panels, dendritic output current (normalized by multiplying by characteristic dendritic resistance  $R_R$ ) is depicted as a function of proximal clamp voltage or reversal potential. The black curves depict the membrane I-V relation (i.e., with the entire membrane clamped at isopotential), the blue curves the dendritic I-V relation under Dirichlet boundary conditions (a proximal voltage clamp), and the red curves the combined I-V relation of the dendrite in parallel with a proximal load (Robin boundary condition). A zero of the current with positive slope on the black or red

curves is indicative of a stable equilibrium; when two such zeros are present, the corresponding system is bistable. Non-unique solutions among the blue curves indicate Dirichlet bistability. Panel *a*: membrane monostable, no Dirichlet bistability, dendrite + load monostable; Panel *b*: membrane monostable, no Dirichlet bistability, dendrite + load bistable; Panel *c*: membrane monostable, Dirichlet bistability, dendrite + load monostable; Panel *d*: membrane monostable, Dirichlet bistability, dendrite + load bistable; Panel *e*: membrane bistable, no Dirichlet bistability, dendrite + load monostable; Panel *f*: membrane bistable, no Dirichlet bistability, dendrite + load bistable; Panel *g*: membrane bistable, Dirichlet bistability, dendrite + load monostable; Panel *h*: membrane bistable, Dirichlet bistability, dendrite + load bistable. The simulation parameters were as follows: Panel *a*:  $\nu = 20$ ,  $\kappa = 6$ ,  $\Lambda = 0.6$ ,  $E_{prox} = -60\text{mV}$ ,  $G_{prox} = 2/R_R$ ; Panel *b*:  $\nu = 20$ ,  $\kappa = 6$ ,  $\Lambda = 0.6$ ,  $E_{prox} = -70\text{mV}$ ,  $G_{prox} = 2/R_R$ ; Panel *c*:  $\nu = 20$ ,  $\kappa = 6$ ,  $\Lambda = 1$ ,  $E_{prox} = -60\text{mV}$ ,  $G_{prox} = 2/R_R$ ; Panel *d*:  $\nu = 20$ ,  $\kappa = 6$ ,  $\Lambda = 1$ ,  $E_{prox} = -80\text{mV}$ ,  $G_{prox} = 2/R_R$ ; Panel *e*:  $\nu = 20$ ,  $\kappa = 9$ ,  $\Lambda = 0.7$ ,  $E_{prox} = -70\text{mV}$ ,  $G_{prox} = 2/R_R$ ; Panel *f*:  $\nu = 20$ ,  $\kappa = 9$ ,  $\Lambda = 0.7$ ,  $E_{prox} = -70\text{mV}$ ,  $G_{prox} = 1/R_R$ ; Panel *g*:  $\nu = 20$ ,  $\kappa = 9$ ,  $\Lambda = 1$ ,  $E_{prox} = -70\text{mV}$ ,  $G_{prox} = 4/R_R$ ; Panel *h*:  $\nu = 20$ ,  $\kappa = 9$ ,  $\Lambda = 1$ ,  $E_{prox} = -70\text{mV}$ ,  $G_{prox} = 1/R_R$ .

In spite of the variety of characteristics associated with the dynamical regimes of this system, some overall trends can be inferred from the results of simulations based on (12), which apply for both Dirichlet and Robin boundary conditions. The range of proximal voltages over which bistability prevails increases with increasing length of the active dendritic segment. For any particular ratio of  $\nu$  and  $\kappa$ ,  $g_{min}$  will increase directly with channel activation, and thus the (non-dimensionalized) critical length decreases inversely with the square root of activation. Additionally, when such a dendrite is bistable, the current delivered to a proximal load depends directly on that level of activation. Finally, as NMDAR activation ( $\nu$ ) increases at a particular level of IRKC activation ( $\kappa$ ), the range of  $E_{prox}$  spanned by the bistable region shifts toward lower potentials, whereas the shift is in the opposite direction when  $\kappa$  increases at fixed  $\nu$ .

As in the single compartment, facilitation and amplifying behavior may be displayed by dendrites with active NMDARs when not in a bistable regime. This may in fact be the normal mode of operation for short dendritic branches whose length and total synaptic input do not support bistable behavior. As NMDARs are activated, the output current and resultant depolarization pass through a high-slope region, and as noted in the previous section, this superlinear response can be exploited to achieve coactivation-dependent facilitation.

The NMDA-induced *dendritic current gain* defined in Methods quantifies the influence of NMDAR activation on the efficacy of other classes of synaptic input, as does membrane resistance in the single compartment. Current gains larger than unity are possible with NMDAR activation. Fig. 7a shows a set of current gain curves for various electrotonic lengths, in a dendrite with NMDARs and without active IRKCs. As in the case of the single compartment, when active IRKCs are present, they have a hyperpolarizing effect but at the same time sharpen the system gain as NMDAR activation increases. Fig. 7b shows examples of current gains at dendritic lengths too short to support bistability, in the space spanned by reversal potential of the load  $E_{prox}$  and the dendritic length  $\Lambda$ , for particular choices of  $\nu$ ,  $\kappa$ , and load conductance. This system is capable of supporting bistability, and current gains are high near limit points (fold bifurcations), and also in a region in parameter space that extends from the point of a cusp bifurcation. Current gains greater than unity demonstrate *power amplification* not just with respect to presynaptic signals, but also with respect to the trans-membrane currents induced by activation of non-NMDA channels, such as AMPA channels.

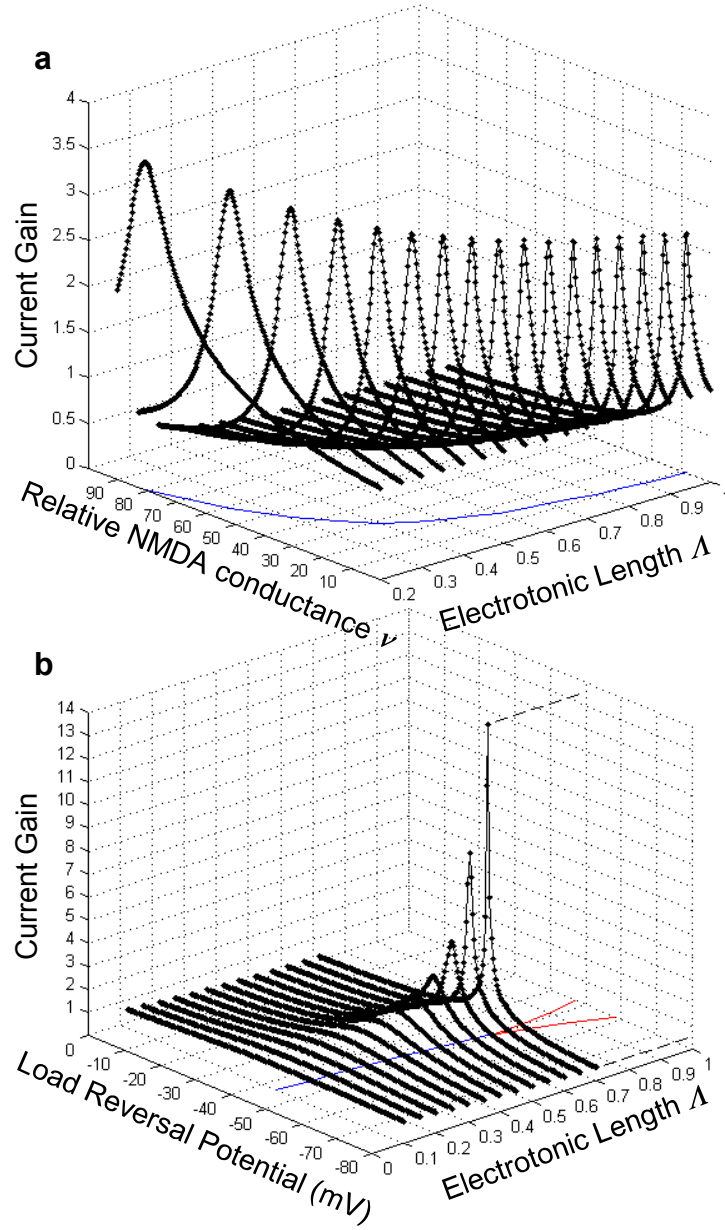


**Fig. 7.** Dendritic output current gains for particular configurations. Panel *a* shows a family of current gain curves as a function of relative NMDAR conductance  $\nu$  and electrotonic length  $\Delta$ , with proximal load conductance  $G_{prox} = 10/R_R$ , and the load reversal potential  $E_{prox} = -70\text{mV}$ . The blue line shows the locus of  $\nu$  values for which the gain is maximum at each value of  $\Delta$ . Panel *b* shows current gains in the space spanned by reversal potential of the load  $E_{prox}$  and the dendritic length  $\Delta$ , with  $\nu=20$ ,  $\kappa = 9$ , and  $G_{prox}$  again equal to  $10/R_R$ . The region outlined in red bounds a bistable regime in this parameter space, and the blue line shows  $E_{prox}$  values corresponding to the maximum gain at each value of  $\Delta$ .

## Neural Multistability

To this point, only bistability in individual dendrites has been examined, but the characteristics of the phenomenon make it clear that it is possible for multiple dendrites on the same neuron to be independently bistable – as pointed out by other authors [8,57],

and demonstrated for dendrites with NMDARs by Korogod and Chernetchenko [46]. This renders the neuron itself a *multistable* entity. Whether or not this is the case for any particular set of dendrites depends on NMDAR (and possibly inward-rectifying potassium channel) activation, the characteristics of the proximal loads, and also the electrical coupling between dendrites due to geometric relationships (i.e., relative positions in a dendritic tree). When individual bistable dendrites are electrically isolated due to physical separation, the capacity for multistability is easily understood. However, for dendrites that terminate in proximity, the assumption of monotonicity of the I-V relation of the proximal load seen by any one dendrite is lost, and their electrical regimes become co-dependent. Nevertheless, it is possible for such dendrites to be independently bistable if their lengths and/or synaptic activations are sufficient. This is demonstrated in simulations of electrically-matched pairs of dendrites terminating proximally at the same electrical node: as either their lengths or the level of coactivation of NMDA and IRKCs increase, the system bifurcates from a monostable to a bistable regime in which both dendrites must assume either the high or low state, and then as length or coactivation increases further, it bifurcates again into a regime with four possible stable states. The same effect applies to larger sets of coupled, electrically-similar dendrites, and it can be regarded as mediating a ‘*variable block voting*’ characteristic: as the level of coactivation increases, the entire set first bifurcates from a monostable to a bistable regime in which all dendrites must assume either the high or low state, then into successive regimes in which progressively larger numbers of stable states are possible, corresponding to the capacity of more and more of the dendrites to reside independently in the high or low state. This is depicted in Fig. 8 for a system of four identical dendrites terminating on a common proximal load. The figure indicates the possible output states of the system by showing the possible values of the proximal membrane potential as the degree of coactivation of NMDARs and IRKCs increases. The bifurcations between and number of stable states in each regime are clearly visible.

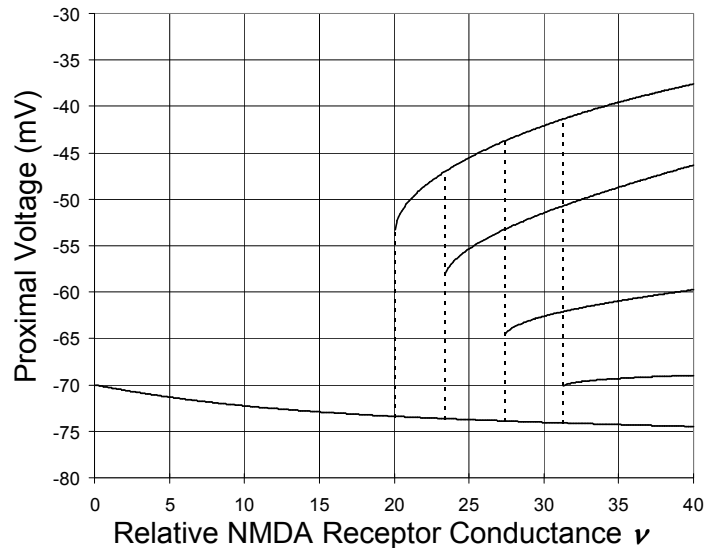


**Fig. 8.** Possible output states of a set of four identical dendrites terminating on a common proximal load, as the degree of coactivation of NMDARs and IRKCs in the dendrites increases. The abscissa indicates NMDAR conductance per unit length  $\nu$  relative to rest in each dendrite; the relative IRKC conductance per unit length  $\kappa$  is maintained in a ratio of 9/20 to  $\nu$ . Electrotonic length of each dendrite is unity. The

ordinate is the voltage appearing at a linear proximal load with conductance  $G_{prox} = 10/R_R$ , and with reversal potential  $E_{prox} = -70\text{mV}$ . Bifurcations from monostable to bistable to multistable regimes are evident.

## Discussion and Conclusions

The results described in the previous section detail the conditions for, and some important characteristics of, amplifying and bistable neural behavior mediated by NMDARs, as revealed by analysis of the stationary equations governing the electrical behavior of model neurons and dendrites. These conditions are physiologically plausible, being consistent with realistic densities of active receptors, and relative conductances of various channels (taking into account the convention for definition of synaptic conductances in the nonlinear models used). During quasistatic traversal of bistable regimes, characteristic phenomena are seen including limit points and hysteresis. As noted by Lazarewicz et al. [41], neural bistability associated with NMDARs requires interaction with other conductances, either in the membrane or cytoplasm. The present results suggest that bistability induced by activation of NMDARs in conjunction with the resting membrane conductance alone is plausible in some classes of neurons, depending on the particular characteristics of the current-voltage relationship of the local NMDAR population, as well as those of the rest state. However, this may be a borderline phenomenon: many neurons are likely to be  $\Gamma$ -monostable with respect to resting conductance, and even when this is not the case, bistability would be expected to prevail for at most a limited range of NMDAR activation levels. Additional hyperpolarizing conductance is necessary for NMDAR-induced bistability in  $\Gamma$ -monostable neurons or neural structures. While in some cases it is conceivable that chloride conductance (e.g., as mediated by  $\text{GABA}_A$  synaptic receptors) could play such a role, the results herein suggest that potassium conductance, in particular, inward-rectifying potassium conductance, is likely to be of greater general significance. As a consequence, the *coactivation of  $\text{GABA}_B$  receptors or SK channels* is seen as a computationally powerful, and in some cases necessary, adjunct condition for NMDAR-mediated bistability.

In addition to bistability, NMDARs can also mediate amplifying behavior. As the density of active receptors in a neuron or neural process increases, the membrane potential eventually passes through a region of relatively rapid depolarization. This nonlinearity can be exploited to achieve coactivation-dependent facilitation, and can also be regarded as setting up an amplifying state, in which current injected by other classes of synaptic receptors has a greater effect on membrane potential than it would in the resting state. As with bistability, it is expected that coactivation of inward-rectifying potassium channels may play a significant role in the characteristics of such amplification. Although active IRKCs have a net hyperpolarizing effect, the interplay between the nonlinear I-V characteristics of NMDARs and IRKCs creates a regime of high incremental membrane resistance that allows rapid transition from hyperpolarized to depolarized states with sufficient activation of depolarizing channels.

Examination of the behavior of dendrites with active NMDARs supports the notion that the dendrite is a critical anatomical locus for information processing. Individual dendrites can display bistable behavior, bifurcating from monostable to bistable regimes as their length, or the activation of NMDAR (and if necessary inward-rectifying potassium) channels in their membrane, increases. The structure of dendrites and the fact that their interiors are not generally at isopotential necessitates the introduction of several

concepts beyond those used in the analysis of single compartment models. *Dirichlet bistability* is defined with respect to the current-voltage relation of a dendrite as a whole, and refers to the existence of two stable values of the output current over some range of imposed clamp voltages at the proximal (or both) ends. *Load-induced bistability* refers to bistability evoked by the influence of a proximal voltage clamp, or electrical load presented by the proximal neural structure, in a dendrite whose membrane would not support bistable behavior if the process were at isopotential. Both phenomena may be observed for physiologically-plausible values of dendritic membrane conductance associated with active NMDAR and inward-rectifying potassium channels.

Individual dendritic segments with approximately uniform membrane conductive properties can display only one or two stable states, but multiple dendrites in a dendritic tree can be independently bistable, rendering the corresponding neuron a multistable entity. A set of bistable dendrites that are closely electrically coupled can also demonstrate a ‘variable block voting’ phenomenon in which, as synaptic activation increases, the set bifurcates from a monostable to a bistable regime in which unanimity is enforced, i.e., two states are possible but all dendrites must assume the same state; then into successive regimes in which larger numbers of dendrites can independently assume different states. This could serve as a mechanism to increase the *resolution* of the state of a neuron as the strength of the synaptic inputs increases, which might be applied, for example, to the extraction of some characteristic of the sensed environment with increasing resolution as confidence in the sensed characteristic increased.

Obviously, NMDAR-induced bistability could subserve short-term memory via persistence of a high or low state entered as a result of the prior history of synaptic activation. However, such a memory primitive is not as simple as the storage of a single bit of information, since the characteristics of the state – e.g., the amount of dendritic output current – can vary with the degree of NMDAR (and IRKC) activation – and thus with time as well. Memory states associated with NMDAR-induced bistability, if they are to endure beyond the time scale of the kinetics of the receptors involved, would require some form tonic activation.

Outside of bistable regimes, amplifying states induced in a dendrite by NMDAR activation may be characterized by a current gain, and current gains substantially larger than unity can be achieved. Coactivation of GABA<sub>B</sub> synapses allows some level of control over the parameters of such amplification. Such control could also be afforded by the influence of adrenergic [76] and cholinergic [77,78] receptors on the properties of SK channels.

A full understanding of the existence and the roles of bistable or amplifying regimes induced by NMDAR activation *in vivo* will require consideration of the dynamics of synaptic inputs and the kinetics of the receptors and ion channels involved. It is noteworthy that NMDAR kinetics are very slow for an ionotropic receptor; the impulse response of channel opening has a time to peak of several tens of milliseconds, roughly an order of magnitude slower than AMPA and GABA<sub>A</sub> receptors [79]. (Also of interest is the fact that GABA<sub>B</sub> kinetics are relatively fast for a metabotropic receptor, such that the time course of activation is only on the order of a factor of two slower than that of NMDARs [79].) This suggests the possibility of scenarios in which a bistable or amplifying regime is set up in a neuron by activation of NMDARs and IRKCs, and rapid changes in state are triggered by other synaptic inputs. (Significant state changes could of

course be induced, with greater time latencies, by changes in NMDA synaptic input as well.) Such scenarios are consistent with observations of amplification and NMDAR-mediated spikes in cortical neurons [11-13,29,30], and apparent dendritic bistability [58]. As noted, more persistent bistable regimes (such as 'up' and 'down' states observed in cortical neurons [9-11,47]), capable of playing a role in short term memory functions, would require tonic activation to maintain, and determining the operating constraints consistent with these regimes would involve joint consideration of mean rates of synaptic activation and receptor kinetics.

Finally, the possible significance of this work for the function of vertebrate neocortical and hippocampal neurons in which NMDARs, AMPA receptors, and SK channels appear together in dendritic spines, and for long-term potentiation (LTP) in such neurons, should be noted. The relative chemical isolation of these spines allows local feedback: activation of glutamatergic synapses induces inward calcium current through NMDARs and the resulting increase in local intracellular calcium activates SK channels, which in turn have an electrical influence on the synaptic channels [53,54]. This influence is often seen as regulating those channels, hyperpolarizing or reducing depolarization of the dendrite and limiting further calcium current. (The *gain* of the feedback loop is effectively modulated by the other receptors mentioned above [76-78], which have an inhibitory effect on SK channels, and this modulated feedback is suspected of playing a role in regulation of LTP.) However, the results presented herein make it clear that SK channel activation could have consequences beyond the hyperpolarizing effects commonly assumed: it could in fact play a role in setting up amplifying or bistable regimes in a dendrite (with modulation of SK channels influencing these regimes). After initial glutamatergic activation, a subsequent surge of input, if sufficiently powerful, could lead to rapid transitions to strongly *depolarized* states, with the transition taking on the characteristics of a thresholding operation as the gain is increased due to the conductance of active SK channels. If a bifurcation to bistability occurs, abrupt transition to depolarized states might require the contribution of fast AMPA receptors to be attained, but these states could linger over the much longer time course of NMDAR activation, which is dictated by its slow kinetics. Such scenarios would lead to additional calcium influx as well as depolarization, and could possibly play some role in the induction of LTP.

It is clear in light of the physiological significance already demonstrated, and the range of computational roles suggested, that further theoretical and numerical study of the electrical effects of NMDARs is merited, particularly in the areas of dynamic behavior and interactions with other nonlinear ion channels in dendritic membranes.

## Acknowledgments

The author thanks Bartlett Mel for discussions and feedback regarding the electrical effects of NMDARs, Andrea Yool for information and references on ion channels, in particular Kir channels, Sean Humbert for comments on dynamical systems aspects of the topic, and Michael Emerling and anonymous reviewers for comments on the manuscript.

This work was supported by U.S. Air Force Office of Scientific Research Grant FA9550-09-1-0116 and U.S. Air Force Research Laboratory Contract FA8651-07-C-0099.

## References

- [1] L. Nowak, P. Bregestovski, P. Ascher, A. Herbert, A. Prochiantz, Magnesium gates glutamate-activated channels in mouse central neurones, *Nature* 307 (1984) 462-465.
- [2] C.E. Jahr, C.F. Stevens, Voltage dependence of NMDA-activated macroscopic conductances predicted by single-channel kinetics, *Journal of Neuroscience* 10 (1990) 3178-3182.
- [3] C.M. Adler, T.E. Goldberg, A.K. Malhotra, D. Pickar, A. Breier, Effects of ketamine on thought disorder, working memory, and semantic memory in healthy volunteers, *Biological Psychiatry* 43 (1998) 811-816.
- [4] J.E. Lisman, J.M. Fellous, X.J. Wang, A role for NMDA-receptor channels in working memory, *Nature Neuroscience* 1 (1998) 273-275.
- [5] X.J. Wang, Synaptic basis of cortical persistent activity: the importance of NMDARs to working memory, *Journal of Neuroscience* 19 (1999) 9587-9603.
- [6] M.J. Rosen, A theoretical neural integrator, *IEEE Transactions on Biomedical Engineering* 19 (1972) 362-367.
- [7] A.A. Koulakov, S. Raghavachari, A. Kepecs, J.E. Lisman, Model for a robust neural integrator, *Nature Neuroscience* 5 (2002) 775-782.
- [8] M.S. Goldman, J.H. Levine, G. Major, D.W. Tank, H.S. Seung, Robust persistent neural activity in a model integrator with multiple hysteretic dendrites per neuron, *Cerebral Cortex* 13 (2003) 1185-1195.
- [9] R. Llinas, M. Sugimori, Electrophysiology of *in vitro* Purkinje cell somata in mammalian cerebellar slices, *Journal of Physiology (London)* 305 (1980) 171-195.
- [10] Y. Loewenstein, S. Mahon, P. Chadderton, K. Kitamura, H. Sompolinsky, Y. Yarom, M. Häusser, Bistability of cerebellar Purkinje cells modulated by sensory stimulation, *Nature Neuroscience* 8 (2005) 202-211.
- [11] S. D. Antic, W.-L. Zhou, A.R. Moore, S.M. Short, K.D. Ikonomu, The decade of the dendritic NMDA spike, *Journal of Neuroscience Research* 88 (2010) 2991-3001.
- [12] R. Lipowsky, T. Gillessen, C. Alzheimer, Dendritic Na channels amplify EPSPs in hippocampal *CA1* pyramidal cells, *Journal of Neurophysiology* 76 (1996) 2181-2191.
- [13] P.C. Schwindt, W.E. Crill, Mechanisms underlying burst and regular spiking evoked by dendritic depolarisation in layer 5 cortical pyramidal neurons, *Journal of Neurophysiology* 81 (1999) 1341-1354.
- [14] P. Heyward, M. Ennis, A. Keller, M.T. Shipley, Membrane bistability in olfactory bulb mitral cells, *Journal of Neuroscience* 21 (2001) 5311-5320.
- [15] A.V. Egerov, B.N. Hamam, E. Fransen, M.E. Hasselmo, A.A. Alonso, Graded persistent activity in entorhinal cortex neurons, *Nature* 420 (2002) 173-178.
- [16] J. Hounsgaard, H. Hultborn, B. Jespersen, O. Kiehn, Intrinsic membrane properties causing a bistable behaviour of alpha-motoneurons, *Experimental Brain Research* 55 (1984) 391-394.
- [17] J. Durand, Synaptic excitation triggers oscillations during NMDAR activation in rat abducent motoneurons, *European Journal of Neuroscience* 5 (1993) 1389-1397.
- [18] O. Kiehn, T. Eken, Functional role of plateau potentials in vertebrate motor neurons, *Current Opinions in Neurobiology* 8 (1998) 746-752.
- [19] W.-C. Li, S.R. Soffe, E. Wolf, A. Roberts, Persistent responses to brief stimuli: feedback excitation among brainstem neurons, *Journal of Neuroscience* 26 (2006) 4026-4035.
- [20] P.C. Schwindt, W.E. Crill, Amplification of synaptic current by persistent sodium conductance in apical dendrite of neocortical neurons, *Journal of Neurophysiology* 74 (1995) 2220-2224.

- [21] R. Lipowsky, T. Gillessen, C. Alzheimer, Dendritic Na channels amplify EPSPs in hippocampal CA1 pyramidal cells, *Journal of Neurophysiology* 76 (1996) 2181-2191.
- [22] M. Mynlieff, K.G. Beam, Characterization of voltage-dependent calcium currents in mouse motoneurons, *Journal of Neurophysiology* 68 (1992) 85-92.
- [23] J. Hounsgaard, O. Kiehn, Calcium spikes and calcium plateaux evoked by differential polarization in dendrites of turtle motoneurons in vivo, *Journal of Physiology (London)* 468 (1993) 245-260.
- [24] J.C. Magee, R.B. Avery, B.R. Christie, D. Johnston, Dihydropyridine-sensitive, voltage-gated  $Ca^{2+}$  channels contribute to resting intracellular  $Ca^{2+}$  concentration of hippocampal CA1 pyramidal neurons, *Journal of Neurophysiology* 76 (1996) 3460-3470.
- [25] N.P. Shapiro, R.H. Lee, Synaptic amplification versus bistability in motoneuron dendritic processing: a top-down modeling approach, *Journal of Neurophysiology* 97 (2007) 3948-3960.
- [26] G.L. Collingridge, C.E. Herron, R.A. Lester, Frequency-dependent N-methyl-D-aspartate receptor-mediated synaptic transmission in rat hippocampus, *Journal of Physiology* 39 (1988) 301-312.
- [27] A. Nicoll, A. Larkman, C. Blakemore, EPSPs in rat neocortical pyramidal neurons in vitro are prolonged by NMDAR-mediated currents, *Neuroscience Letters* 143 (1992) 5-9.
- [28] A.M. Thomson, Activity-dependent properties of synaptic transmission at two classes of connections made by rat neocortical pyramidal axons *in vivo*, *Journal of Physiology (London)* 502 (1997) 131-147.
- [29] J. Schiller, G. Major, H.J. Koester, Y. Schiller, NMDA spikes in basal dendrites of cortical pyramidal neurons, *Nature* 404 (2000) 285-289.
- [30] J. Schiller, Y. Schiller, NMDAR-mediated dendritic spikes and coincident signal amplification, *Current Opinions in Neurobiology* 11 (2001) 343-348.
- [31] J. Kalliomaki, M. Granmo, J. Schouenborg, Spinal NMDA-receptor dependent amplification of nociceptive transmission to rat primary somatosensory cortex (SI), *Pain* 104 (2003) 195-200.
- [32] A. Polsky, B.W. Mel, J. Schiller, Computational subunits in thin dendrites of pyramidal cells, *Nature Neuroscience* 7 (2004) 621-627.
- [33] T. Nevian, M.E. Larkum, A. Polsky, J. Schiller, Properties of basal dendrites of layer 5 pyramidal neurons: a direct patch-clamp recording study, *Nature Neuroscience* 10 (2007) 206-214.
- [34] S. Cash, R. Yuste, Linear summation of excitatory inputs by CA1 pyramidal neurons, *Neuron* 22 (1999) 383-394.
- [35] B.W. Mel, Information processing in dendritic trees, *Neural Computation* 6 (1994) 1031-1085.
- [36] A.B. MacDermott, M.L. Mayer, G.L. Westbrook, S.J. Smith, J.L. Barker, NMDA-receptor activation increases cytoplasmic calcium concentration in cultured spinal cord neurones, *Nature* 321 (1986) 519-522.
- [37] R. Schneggenberger, Z. Zhou, A. Konnerth, E. Neher, Fractional contribution of calcium to the cation current through glutamate receptor channels, *Neuron* 11 (1993) 133-143.
- [38] R.A. North, T. Tokimasa, Persistent calcium-sensitive potassium current and the resting properties of guinea-pig myenteric neurones, *Journal of Physiology* 386 (1986) 333-353.
- [39] J.L. Calton, M.H. Kang, W.A. Wilson, S.D. Moore, NMDAR-dependent synaptic activation of voltage-dependent calcium channels in basolateral amygdala, *Journal of Neurophysiology* 83 (2000) 685-692.
- [40] B.W. Mel, Synaptic integration in an excitable dendritic tree, *Journal of Neurophysiology* 70 (1993) 1086-1101.
- [41] M.T. Lazarewicz, C.-W. Ang, G.C. Carlson, D.A. Coulter, L.H. Finkel, Analysis of NMDA-dependent voltage bistability in thin dendritic compartments, *Neurocomputing* 69 (2006) 1025-1029.
- [42] B.W. Mel, NMDA-Based pattern discrimination in a modeled cortical neuron, *Neural Computation* 4 (1992) 502-516.

- [43] B.W. Mel, D.L. Ruderman, K.A. Archie, Translation-invariant orientation tuning in visual 'complex' cells could derive from intradendritic computations, *Journal of Neuroscience* 18 (1998) 4325-4334.
- [44] K.A. Archie, B.W. Mel, A model for intradendritic computation of binocular disparity, *Nature Neuroscience* 3 (2000), 54-63.
- [45] S.M. Korogod, I.B. Kulagina, Electrical bistability in a neuron model with monostable dendritic and axosomatic membranes, *Neurophysiology* 32 , (2000) 73-76.
- [46] S.M. Korogod, D.V. Chernetchenko, Nature of electrical tristability in a neuron model with bistable asymmetrical dendrites, *Neurophysiology* 40 (2008) 412-416.
- [47] J.A. Wolf, J.T. Moyer, L. Finkel, The role of NMDA currents in state transitions of the nucleus accumbens medium spiny neuron, *Neurocomputing* 65-66 (2005) 565-570.
- [48] S. Wright, Generation of resting membrane potential, *Advanced Physiology Education* 28 (2004) 139-142.
- [49] D.D. Mott, D.V. Lewis, The Pharmacology and Function of Central GABA<sub>B</sub> Receptors, Ch. 4 in: *International Review of Neurobiology* Vol. 36., R.J. Bradley, R.A. Harris (Eds.), 1994, pp. 97-224.
- [50] D.L. Sodickson, B.P. Bean GABA<sub>B</sub> receptor-activated inwardly rectifying potassium current in dissociated hippocampal CA3 neurons, *Journal of Neuroscience* 16 (1996) 6374-6385.
- [51] K. Kaupmann, V. Schuler, J. Mosbacher, S. Bischoff, et al. Human gamma-aminobutyric acid type B receptors are differentially expressed and regulate inwardly rectifying K<sup>+</sup> channels, *Proceedings of the National Academy of Sciences U S A* 95 (1998) 14991-6.
- [52] C.E. Fowler, P. Aryal, K.F. Suen, P.A. Slesinger, Evidence for association of GABA(B) receptors with Kir3 channels and regulators of G protein signalling (RGS4) proteins, *Journal of Physiology* 580 Pt 1 (2007) 51-65.
- [53] J.T. Ngo-Anh, B.L. Bloodgood, M. Lin, B.L. Sabatini, J. Maylie, J.P. Adelman, SK channels and NMDA receptors form a Ca<sup>2+</sup>-mediated feedback loop in dendritic spines, *Nature Neuroscience* 8 (2005) 642-649.
- [54] B.L. Bloodgood, B.L. Sabatini, Regulation of synaptic signalling by post-synaptic, non-glutamate receptor ion channels, *Journal of Physiology* 586.6 (2008) 1475-1480.
- [55] B. Lancaster, R.A.N. Nicoll, D. J. Perkel, Calcium activated two types of potassium channels in rat hippocampal neuron in culture, *Journal of Neuroscience* 11 (1991) 23-30.
- [56] H. Soh and C.-S. Park, Inwardly rectifying current-voltage relationship of small-conductance Ca<sup>2+</sup>-activated K<sup>+</sup> channels rendered by intracellular divalent cation blockade, *Biophysical Journal* 80 (2001) 2207-2215.
- [57] A. Gutman, Nerve cell dendrites. Theory, electrophysiology, function. (Russian), Mokslas, Vilnius, 1984, pp. 9-126.
- [58] A. Gutman, Bistability of dendrites, *International Journal of Neural Systems* 1 (1991) 291-304.
- [59] D.E. Goldman, Potential, impedance, and rectification in membranes, *Journal of General Physiology* 27 (1943) 37-60.
- [60] A.L. Hodgkin, B. Katz. The effect of sodium ions on the electrical activity of the giant axon of the squid, *Journal of Physiology* 108 (1949) 37-77.
- [61] C. Koch, *Biophysics of computation: Information processing in single neurons*. Oxford University Press, New York, Oxford, 1999.
- [62] A.J. Watt, M.C.W. van Rossum, K.M. MacLeod, S.B. Nelson, G.G. Turrigiano, Activity Coregulates Quantal AMPA and NMDA Currents at Neocortical Synapses, *Neuron* 26 (2000) 659-670.
- [63] W. Rall, The theoretical foundation of dendritic function: Selected papers of Wilfred Rall with commentaries, in: I. Segev, J. Rinzel, G.M. Shepherd (Eds.), MIT Press, Cambridge, MA, 1995.

- [64] G. Nyíri, F.A. Stevenson, T.F. Freund, P. Somogyi, Large variability in synaptic N-methyl-D-aspartate receptor density on interneurons and a comparison with pyramidal-cell spines in the rat hippocampus, *Neuroscience* 119 (2003) 347-363.
- [65] H.R. Santos, W.M. Cintra, Y. Aracava, C.M. Maciel, N.G. Castro, E.X. Albuquerque, Spine density and dendritic branching pattern of hippocampal CA1 pyramidal neurons in neonatal rats chronically exposed to the organophosphate paraoxon, *Neurotoxicology* 25 (2004) 481-494.
- [66] N. Hájos, T.F. Freund, I. Mody, Comparison of single NMDAR channels recorded on hippocampal principal cells and oriens/alveus interneurons projecting to stratum lacunosum-moleculare (O-LM cells), *Acta Biologica Hungarica* 53 (2002) 465-472.
- [67] Y.A. Kusnetsov, *Elements of applied bifurcation theory*, Springer, New York, 1995.
- [68] S.H. Strogatz, *Nonlinear dynamics and chaos, with applications to physics, biology, chemistry, and engineering*, Westview Press, Cambridge, MA, 1994.
- [69] A.L. Buller, H.C. Larson, B.E. Schneider, J.A. Beaton, et al., The molecular basis of NMDAR subtypes: Native receptor diversity is predicted by subunit composition, *Journal of Neuroscience* 14 (1994) 5471-5484.
- [70] P. Rhodes, The properties and implications of NMDA spikes in neocortical pyramidal cells, *Journal of Neuroscience* 26 (2006) 6704-6715.
- [71] J.M. Bekkers, C.F. Stevens, NMDA and non-NMDARs are co-localized at individual excitatory synapses in cultured rat hippocampus, *Nature* 341 (1989) 230-233.
- [72] G.F. Tseng, L.B. Haberly, Characterization of synaptically-mediated fast and slow inhibitory processes in piriform cortex in an *in vitro* slice preparation, *Journal of Neurophysiology* 60 (1988) 1352-1376.
- [73] P. Butrimas, A. Gutman, Theoretical input current-voltage characteristics of the neuron with NC-dendrites on uniform shift of the clamped potential of the soma, *Biophysics-USSR* 26 (1981) 340-345.
- [74] A. Alaburda, M. Alaburda, A. Baginskas, A. Gutman, G. Svirskis, Criteria of bistability of the cylindrical dendrite with variable negative slope of N-shaped current-voltage (I-V) membrane characteristic, *Biophysics-USSR* 46 (2001) 337-340.
- [75] A. Gutman, A. Baginskas, J. Hounsgaard, N. Svirskiene, G. Svirskis, Semi-quantitative theory of bistable dendrites with potential-dependent facilitation of inward current, in: G.N. Reeke, R.R. Poznanski, K.A. Lindsay, J.R. Rodenberg, O. Sporns (Eds.), *Modeling in the neurosciences: From biological systems to neuromimetic robots*, Taylor & Francis, Boca Raton, London, New York, Singapore, 2005, pp. 435-457.
- [76] E.S.L. Faber, A.J. Delaney, J.M. Power, P.L. Sedlak, J.W. Crane, P. Sah, Modulation of SK Channel Trafficking by Beta Adrenoceptors Enhances Excitatory Synaptic Transmission and Plasticity in the Amygdala, *Journal of Neuroscience* 28 (2008) 10803-10813.
- [77] A.J. Giessel, B.L. Sabatini, M1 muscarinic receptors boost synaptic potentials and calcium influx in dendritic spines by inhibiting postsynaptic SK channels, *Neuron* 68 (2010) 936-947.
- [78] K.A. Buchanan, M.M. Petrovic, S.E. Chamberlain, N.V. Marrion, J.R. Mellor, Facilitation of long-term potentiation by muscarinic M(1) receptors is mediated by inhibition of SK channels, *Neuron* 68 (2010) 948-963.
- [79] A. Destexhe, Z. Mainen, T.J. Sejnowski, Synthesis of models for excitable membranes, synaptic transmission, and neuromodulation using a common kinetic formalism, *Journal of Computational Neuroscience* 1 (1994) 195-230.